JOURNAL OF BACTERIOLOGY, Mar. 2005, p. 1913–1922 Vol. 187, No. 6
0021-9193/05/$08.00+0 doi:10.1128/JB.187.6.1913–1922.2005

Helical Disposition of Proteins and Lipopolysaccharide in the Outer Membrane of *Escherichia coli*

Anindya S. Ghosh† and Kevin D. Young*

Department of Microbiology and Immunology, University of North Dakota School of Medicine and Health Sciences, Grand Forks, North Dakota

Received 22 October 2004/Accepted 3 December 2004

In bacteria, several physiological processes once thought to be the products of uniformly dispersed reactions are now known to be highly asymmetric, with some exhibiting interesting geometric localizations. In particular, the cell envelope of *Escherichia coli* displays a form of subcellular differentiation in which peptidoglycan and outer membrane proteins at the cell poles remain stable for generations while material in the lateral walls is diluted by growth and turnover. To determine if material in the side walls was organized in any way, we labeled outer membrane proteins with succinimidyl ester-linked fluorescent dyes and then grew the stained cells in the absence of dye. Labeled proteins were not evenly dispersed in the envelope but instead appeared as helical ribbons that wrapped around the outside of the cell. By staining the O8 surface antigen of *E. coli* 2443 with a fluorescent derivative of concanavalin A, we observed a similar helical organization for the lipopolysaccharide (LPS) component of the outer membrane. Fluorescence recovery after photobleaching indicated that some of the outer membrane proteins remained freely diffusible in the side walls and could also diffuse into polar domains. On the other hand, the LPS O antigen was virtually immobile. Thus, the outer membrane of *E. coli* has a defined in vivo organization in which a subfraction of proteins and LPS are embedded in stable domains at the poles and along one or more helical ribbons that span the length of this gram-negative rod.

The idea that bacteria might be no more than small sacks of enzymes and substrates mixed together in an amorphous jumble has given way to the realization that many proteins, processes, and macromolecules have geometrically diverse locations and exhibit asymmetric behaviors. One example of this changing concept is that in *Escherichia coli* the cell poles can be considered to be distinctive organelles in which neither peptidoglycan nor outer membrane (OM) proteins are recycled or diluted (9, 10, 12, 26). Numerous proteins or physiological complexes congregate exclusively at one or both poles, with implications for protein secretion, environmental sensing, cellular development, virulence, and gene transfer (14, 19, 31, 54, 55). Furthermore, one or more of these asymmetries may regulate bacterial morphology because inaccurate localization of extraneous pole-like domains produces cells with aberrant shapes (12, 44).

Another surprising facet of prokaryotic structure is that several proteins assemble in long filaments that spiral across the inner face of the cytoplasmic membrane, reaching from one end of the cell to the other. The MreB and Mbl proteins form such fibrils, or cables, in *Bacillus subtilis* (22) and *Caulobacter crescentus* (17) and may serve as internal scaffolds that position peptidoglycan-synthesizing enzymes, thereby defining the shape of the cell wall (17, 29, 33). The MinCD proteins oscillate from pole to pole along helical paths, inhibiting polymerization of the principal cell division protein FtsZ and helping to define the cell's center (56). FtsZ itself moves from completed septa to new division sites by traveling along helical pathways on the inner membrane (1, 58), and even nonassembled FtsZ monomers oscillate back and forth along helical tracks (60). DNA dispersal at cell division also relies on proteins with helical distributions: the SetB protein is required for proper chromosomal segregation in *E. coli* (16), and the ParA protein moves along spiral-shaped threads to segregate R1 plasmids (13). And finally, the SecA and SecY secretion complexes are distributed in helical fashion in the inner membrane of *B. subtilis* (4), although this may not be true in *E. coli* (3). Except for the Sec proteins, the other spiraling proteins seem to share the common function of partitioning some substance—shape elements (MreB and Mbl), cell volume (MinCD and FtsZ), or DNA (SetB and ParA)—so that the materials are distributed uniformly to daughter cells after division.

One question that arises is whether one of the above proteins creates the principal scaffold on which the others assemble or travel, or if there is an underlying helical structure in which proteins move independently. A recent observation hints at the importance of the latter possibility. Gibbs et al. found that in *E. coli* newly synthesized LamB protein diffuses throughout the OM in a helical fashion (20). This behavior implies the existence of long-lived spiral boundaries that restrict the diffusion of LamB, and perhaps other surface proteins, to defined OM "canals." However, the OM has been considered to be continuous and homogeneous, and no obvious structure has been observed that might serve such a purpose. On the other hand, polar domains constitute an exception to the idea of the uniformity of the OM (9, 12). Since an unknown mechanism maintains this distinction between the poles and the cell cylinder, another overlooked structure(s) may exist in the cell envelope as well.

In this work we ask whether components of the OM have

* Corresponding author. Mailing address: Department of Microbiology and Immunology, University of North Dakota School of Medicine and Health Sciences, Grand Forks, ND 58202-9037. Phone: (701) 777-2624. Fax: (701) 777-2054. E-mail: kyoung@medicine.nodak.edu.

† Present address: Department of Biotechnology, Indian Institute of Technology, Kharagpur 721302, West Bengal, India.

TABLE 1. *E. coli* strains used in this study

Strain	Genotype	O antigen[a]	ConA-AF488 binding[b]	Source
CS109	W1485 *rpoS rph*	None	−	C. Schnaitman
KL743	MG1655 *zba-3000*::Tn*10* LAM$^-$ *rph*	None	−	M. Goldberg (CGSC 6213)
2443	*thr-1 leuB6* Δ(*gpt-proA*)*66 argE3 thi-1 rfb*$_{O8}$ *lacYl ara-14 galK2 xyl-5 mtl-1 mgl-51 rpsL31 kdgK51*	O8	+	A. T. Maurelli (35)
2443T	2443 *zba-3000*::Tn*10* (Tet^r) (by P1 transduction from KL743)	O8	+	This work
AG430-2K	2443 *hisI*::*npt* (Kan^r) *rfb*$_{K-12}$	None	−	This work
AGTO2-1K	2443T (Tet^r) *hisI*::*npt* (Kan^r) *rfb*$_{K-12}$	None	−	This work
JM105	*thi-1 rpsL endA sbcBC hsdR4* Δ(*lac-pro*) (*F′ traD36 proAB lacI*^{q}*Z*ΔM15)	None	−	S. Detke
KM32	*leuB6 proA2 thr-1 argE3 lacY1 galK2 ara-14 xyl-5 thi-1 rpsL31 mtl-1 tsx-33 supE44* Δ(*recC ptr recB recD*)::P_{lac}-*bet exo* (Cam^r)	None	−	K. C. Murphy (41)
KM32I-9	KM32 *hisI*::*npt* (Kan^r) (by λRed recombination)	None	−	This work

[a] Detected by SDS-PAGE.
[b] Detected by fluorescence microscopy.

geometric distributions different from that expected to occur by random dispersal. When either protein or lipopolysaccharide (LPS) was labeled with a fluorescent compound and then chased by growing cells in the absence of label, stained material was organized in stable helical swaths. These data, combined with previous observations, suggest that the gram-negative cell envelope has a stable and innate helical property that includes all of its components: peptidoglycan, proteins, and lipids.

MATERIALS AND METHODS

Bacteria, plasmids, and general techniques. The bacterial strains used in this study are listed in Table 1. Plasmid pBMM1 (34) was constructed by ligating the 2.123-kb EcoRI-HindIII fragment containing the *res-npt-res* kanamycin resistance-encoding cassette from pCK155 (28) into the EcoRI-HindIII sites of pBCSK (Stratagene, La Jolla, Calif.). Bacteria were grown in Luria-Bertani (LB) broth, on LB agar plates, or in M9 minimal glucose medium (37) supplemented with 40 μg of amino acids (L-threonine, L-leucine, L-arginine, L-lysine, and L-histidine) per ml. Where appropriate, antibiotics were added to the following concentrations: ampicillin, 100 μg/ml; chloramphenicol, 20 μg/ml; kanamycin, 50 μg/ml; tetracycline, 25 μg/ml. When indicated, aztreonam, a specific inhibitor of penicillin binding protein 3, was added to cultures at a final concentration of 5 μg/ml. Unless otherwise specified, chemicals and reagents were purchased from Sigma Chemical Co. (St. Louis, Mo.).

Deletion of the *hisI* gene. The chromosomal *hisI* gene was deleted and replaced with a kanamycin resistance cassette from plasmid pBMM1. pBMM1 was digested with EcoRI and HindIII, and a 2.5-kb DNA fragment was purified. With this fragment as a template, the kanamycin resistance cassette was amplified by using a pair of primers, the 3′ ends of which consisted of a 20-nucleotide sequence complementary to either the 5′ or 3′ end of the *npt* gene. To each of these was added a 49-nucleotide sequence complementary to chromosomal sequences adjacent to the *hisI* gene. The complete primer sequences were 5′-GCA AAG TCA CCT TCT TCT CGC GCA CTA AAC AGC GAC TGT GGA CCA AAG GCG TGG GCG AAG AAC TCC AGC-3′ and 5′-CGG CAG ATT TGC GCT CGG CGA GCA GTT GTT CCA GTT GAT ACA GGA ACA GCG TGC TAA TGT GGT TAC GTG-3′. PCR amplification was initiated by a single melting step of 94°C for 5 min, followed by 30 amplification cycles (94°C for 1 min, 65°C for 1 min, 72°C for 1 min), concluding with a single incubation at 72°C for 7 min. The resulting 1.5-kb PCR fragment was purified by using a gel extraction kit (QIAGEN Inc., Valencia, Calif.) and electroporated into *E. coli* KM32, where the chromosomal *hisI* gene was replaced with the antibiotic cassette via λRed recombination (41). Recombinants were selected by plating on LB medium plus kanamycin and screened for the inability to grow in histidine-deficient minimal medium. The presence of the *hisI* deletion in strain KM32I-9 was confirmed by diagnostic PCR. This *hisI*::Kan^r allele and the neighboring *rfb* locus from *E. coli* K-12 were cotransduced into *E. coli* 2443 by P1 transduction (36) to create strain AG430-2K, which formed rough colonies and lacked a complete O antigen.

LPS preparation. LPS was extracted by the method of Hitchcock and Brown (21), with minor modifications. Cells were incubated in 1.5 ml of LB medium overnight at 37°C, harvested by centrifugation, washed with 1 ml of 0.1 M phosphate-buffered saline (PBS; pH 7.4), and resuspended in 1 ml of PBS. To this suspension was added 50 μl of lysis buffer consisting of 1 M Tris-HCl (pH 6.8) containing 2% sodium dodecyl sulfate (SDS), 4% β-mercaptoethanol, 10% glycerol, and bromophenol blue. Cells were lysed by boiling for 10 min, proteinase K was added to a final concentration of 500 μg/ml, and the samples were incubated at 60°C for 60 min, mixed well, and centrifuged at 14,000 × *g* to remove cell debris. Samples (10 μl) were loaded onto a 12% polyacrylamide gel (iGels; Gradipore Ltd., Frences Forest, Australia), and LPS was separated by electrophoresis at a 35-mA constant current. Gels were stained with the Pro-Q Emerald 300 LPS gel stain kit (Molecular Probes Inc., Eugene, Oreg.) in accordance with the manufacturer's instructions. A commercial LPS preparation from *E. coli* serotype O55:B5 (Sigma Chemical Co.) was loaded onto each gel as a control.

Labeling of OM proteins. *E. coli* OM proteins were labeled with succinimidyl ester (NHS)-Texas red or NHS–Alexa-Fluor 488 (NHS-AF488) (Molecular Probes, Inc.) as previously described (9, 12). In brief, bacteria were incubated at 37°C in LB broth to an optical density at 550 nm (OD_{550}) of 0.7, washed twice with sodium bicarbonate buffer (0.1 M, pH 8.0), and stained with NHS-Texas red (final concentration, 100 μg/ml) or NHS-AF488 (50 μg/ml). Stained cells were washed three times with bicarbonate buffer, diluted in LB broth, and incubated at 37°C with or without aztreonam in the absence of the dye. Samples were withdrawn after various time intervals, fixed with 0.5% formalin, and visualized by phase and fluorescence microscopy.

ConA labeling of LPS O8 polysaccharide. Bacterial cultures were grown in LB medium to an OD_{550} of 0.7, harvested by centrifugation, washed twice with 0.1 M PBS, and resuspended in one-third volume of PBS. Concanavalin A (ConA)-conjugated Alexa-Fluor 488 (ConA-AF488; Molecular Probes, Inc.) was dissolved in PBS (pH 7.4) to give a 5-mg/ml stock solution. ConA-AF488 was added to the cell suspension to give a final concentration of 200 μg/ml, and the mixture was incubated in the dark at room temperature for 30 min with gentle shaking. Stained cells were washed twice and resuspended in PBS for microscopy. For chase experiments, a 250-μl volume of stained cells was inoculated into 10 ml of LB medium and incubated at 37°C in the dark and aliquots were withdrawn at intervals for microscopy.

Double labeling. Proteins and LPS in the same cells were labeled in a two-step procedure. *E. coli* 2443 was grown to an OD_{600} of ~0.7, and 3 ml of cells was pelleted, washed twice with 0.1 M sodium bicarbonate buffer (0.1 M, pH 8.0), and resuspended in 1 ml of the same buffer. NHS-AF488 was added to a final concentration of 50 μg/ml, and the mixture was incubated for 30 min at room temperature in the dark. The cells were then washed twice with 0.1 M PBS, pH 7.4, and either ConA-AF488 or unlabeled ConA (ICN Biomedical Inc., Irvine, Calif.) was added to a final concentration of 200 μg/ml. The suspension was incubated at room temperature in the dark for 30 min, washed twice with 0.1 M PBS (pH 7.4), and subjected to fluorescence microscopy or fluorescence recovery after photobleaching (FRAP).

Labeling of inner membrane. The inner membrane was stained with the dye FM4-64 as previously described (18). Briefly, cells were incubated at 37°C in LB

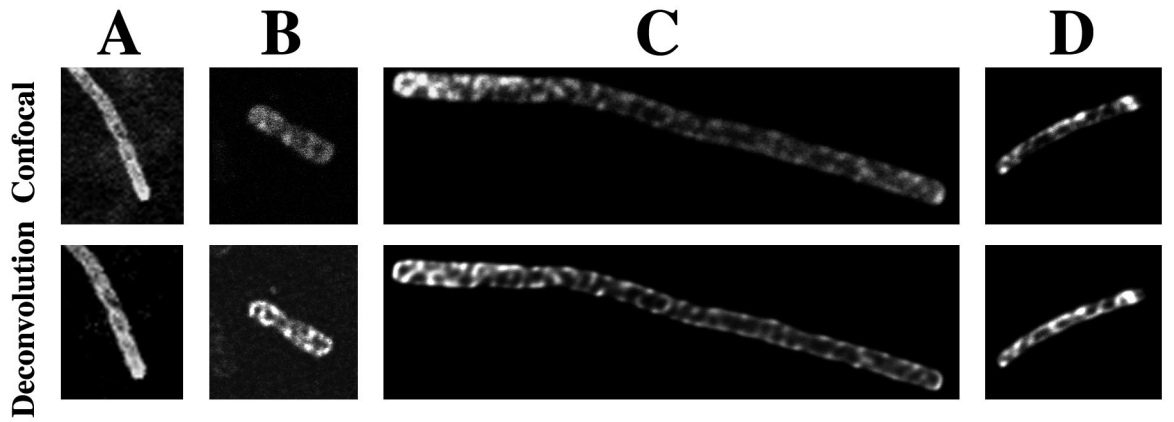

FIG. 1. Pulse-chase visualization of OM protein helices in *E. coli*. OM proteins were labeled with NHS-Texas red or NHS-AF488. Stained cells were grown at 37°C in the absence of label, harvested, and visualized by confocal microscopy. In some cases, cells were forced to filament before and during the chase by adding aztreonam, which inhibits penicillin binding protein 3, an essential septation protein. Cells are presented as the original confocal picture or as processed by deconvolution. (A) *E. coli* CS109 elongated with aztreonam for 120 min, stained with NHS-Texas red, and chased for 120 min. (B) Nonelongated *E. coli* CS109 stained with NHS-Texas red and chased for 120 min. (C) *E. coli* CS109 elongated with aztreonam for 60 min, stained with NHS-Texas red, and chased for 120 min. (D) *E. coli* 2443 elongated with aztreonam, stained with NHS-AF488, and chased for 60 min.

broth to an OD_{550} of 0.7, harvested by centrifugation, washed twice with 0.1 M PBS (pH 7.4), and resuspended in one-third volume of PBS. FM4-64 (Molecular Probes, Inc.) in dimethyl sulfoxide was added to give a final concentration of 4 μg/ml, and the mixture was incubated in the dark at room temperature for 30 min with gentle shaking. Stained cells were washed twice with PBS and resuspended in PBS for microscopy. For chase experiments, 250 μl of stained cells was inoculated into 10 ml of LB medium with or without aztreonam and incubated in the dark at 37°C and aliquots were withdrawn at 30, 60, or 90 min for microscopy.

Microscopy. Cell suspensions (5 μl) were placed on microscope slides coated with 1% agarose and incubated at room temperature for 10 min to immobilize the cells. Light microscopy was performed by viewing cells with a 100× oil immersion objective on a Nikon OPTIPHOT-2. AF488-labeled and Texas red-labeled compounds were detected by using either a fluorescein isothiocyanate filter (470-nm excitation, 530- and 550-nm emission) or a rhodamine filter (595-nm excitation, 615-nm emission), respectively (Chroma Technology Corp., Rockingham, Vt.). Images were captured with a black-and-white Pixera Penguin 600CLM cooled charge-coupled device camera controlled by Image-Pro Plus software (Media Cybernetics, Silver Spring, Md.).

Confocal microscopy and FRAP. FRAP was performed on cells labeled with either NHS-AF488 (for *E. coli* CS109 or 2443) or ConA-AF488 (for *E. coli* 2443). Overnight cultures in LB medium were diluted 1:100 into 10 ml of LB medium and incubated for 1 h, after which aztreonam was added (to 5 μg/ml) and the cells were grown for about four generations to an OD_{550} of 0.7. Cells to be labeled with ConA-AF488 were harvested by centrifugation and washed with 0.1 M PBS (pH 7.4); those to be stained with NHS-AF488 were washed with 0.1 M sodium bicarbonate buffer (pH 8.0). Each wash buffer contained aztreonam (5 μg/ml). At this point, the cells were labeled with either ConA-AF488 (200 μg/ml) or NHS-AF488 (50 μg/ml) and incubated for 30 min at room temperature in the dark with gentle shaking. Labeled cells were washed twice with the respective buffers containing aztreonam, and 2 μl of cell suspension was spotted onto the surface of 0.3% agar squares of LB medium-aztreonam in Lab-Tek chamber slides (Nalge Nunc International, Naperville, Ill.) or, in some cases, onto polylysine-coated slides. A coverslip was applied, and the cells were observed by confocal microscopy. In some experiments, labeled cells were chased by incubating dilutions in LB medium or PBS (pH 7.2) and microscopy and FRAP analysis were performed on samples harvested at 30-min intervals over the course of 2.5 h.

Confocal microscopy was performed with a microscope (model LSM510 Meta; Zeiss, Jena, Germany) fitted with a 100× 1.45 N.A. plan-fluar objective and driven by Zeiss AIM software. The procedure was a modified version of the method described by Cowan et al. (6). Two to five prebleach images of each microscopic field were photographed, after which a small portion of a cell filament was circumscribed for bleaching. The size of the bleach area was set so that its diameter was ~30% greater than the width of the filament. Each cell segment was bleached by exposing the area for 20 to 50 iterations (2 to 4 s total) to the 488-nm line of an argon laser (30-mW maximum power, 6.1-A tube current). Fluorescence recovery was documented by photographing the cell every 5 s for 5 to 10 min after photobleaching. Images were visualized with the Zeiss LSM image browser, deconvolution was performed with AutoDeblur Gold CF 9.3.2 and the AutoVisualize program (Autoquant, Watervliet, N.Y.), and image processing and analysis of fluorescence recovery were performed with the Image J program (National Institutes of Health, Bethesda, Md.). For the latter analyses, the average background value of a cell-free area was subtracted from each image.

RESULTS

Some proteins are arranged in helical ribbons in the OM. Cell poles in wild-type *E. coli* and the poles and deformities in shape-defective mutants retain stable patches of OM proteins after prolonged growth (9, 12). Fluorescence light microscopy easily detected labeled proteins in these relatively large regions, but there were hints that the cells also contained thread-like strings of stable proteins in their lateral walls as well. To test this possibility more rigorously, we used confocal microscopy to follow the fate of OM proteins.

Proteins in the OMs of *E. coli* CS109 and 2443 were labeled with NHS-Texas red or NHS-AF488, after which the cells were incubated in the absence of the stain and visualized by confocal microscopy. As expected, proteins labeled by either dye remained in stable patches at the poles after the chase period, but in addition, broad helical strings of stable material also appeared in the lateral walls (Fig. 1). In all of the cells examined, these helices were embedded in a light background of evenly distributed fluorescence (Fig. 1, upper row), implying that some proteins were free to diffuse while others were immobile. The helical distribution was visible by simple inspection but was most easily discerned by assembling a series of *z* stack photographs taken in successive planes and then sharpening the pictures by deconvolution (Fig. 1, lower row). These steps effectively subtracted the hazy background contributed by uniformly distributed proteins. The stable structures appeared to consist of at least two intertwining ribbons, and although many helices seemed more prominent near the poles, most

filaments exhibited helical distributions along their entire length (Fig. 1). We conclude that at least some *E. coli* OM proteins are arranged in stable helical structures that persist in the face of diffusion and insertion of new material, indicating that these proteins are either immobile or poorly mobile.

There are no inherent diffusion barriers in the OM or inner membrane. One explanation for stable protein groupings in the OM is that such patches arise because they are trapped in lipid domains that are so tightly sequestered from one another that diffusion between domains is restricted or prevented. We tested this proposition by labeling OM proteins with NHS-AF488 and using FRAP to measure protein diffusion in the OMs of living cells. In every case, the bleached areas recovered fluorescence within 10 to 40 s (Fig. 2A to C and 3A to C), indicating that proteins in neighboring portions of the membrane were mobile. Fluorescence recovery occurred not only in the lateral walls but also at the poles (Fig. 2C and 3C), although the rate and extent of recovery might have been very slightly lower (compare Fig. 3C to Fig. 3A and B). The results indicate that no mechanical obstructions prevented protein diffusion into broad areas of the wall or poles. In particular, proteins diffused uniformly into the bleached areas of elongated cells and no helical structures were reconstituted (Fig. 2A to C), suggesting that the diffusible proteins were not part of stable helices.

Although there were no impenetrable barriers to diffusion within the OM, it was possible that such barriers exist in the inner membrane. To test this, we stained cells with the lipophilic dye FM4-64, which preferentially stains the inner membrane (18), and chased the label by growing the cells in the absence of dye. If diffusion was mechanically restricted by variation in lipid composition or behavior, then a portion of the dye should be trapped in domains limited to the poles or helical formations in the side walls, whereas fluorescence in the rest of the cell would be diluted by growth. A uniform distribution of FM4-64 would indicate that diffusion was unimpeded by natural lipid barriers. The latter result was observed (Fig. 4). All cells displayed uniform fluorescence around their peripheries, indicating that there were no barriers to diffusion among inner membrane domains over the poles or in the lateral walls.

Specific labeling of LPS O antigen. The outer leaflet of the OM of gram-negative bacteria is composed of LPS (48, 49). Even though proteins diffused freely in this environment, the LPS itself could be distributed in one of two ways. LPS might simply be an inert, randomly diffusing matrix in which the immobile protein helices were embedded, or else a portion of the LPS might also be stable and immobile. To distinguish between these possibilities, we labeled the O-antigen side chain of *E. coli* 2443 with ConA-AF488, a fluorescent lectin that binds specifically to α-glucose and α-mannose residues of the O8 antigen present in this strain (5, 8).

E. coli 2443 labeled with ConA-AF488 exhibited an evenly distributed fluorescence around the cell periphery (Fig. 5A). The interaction between dye and cells was quite stable: ConA was not washed away by repeated rinsing with 0.1 M PBS (pH 7.4), and cells retained their fluorescence after being incubated for 90 min in PBS in the absence of free ConA-AF488 (not shown). Staining intensity decreased only when labeled cells were stored for 7 days in the dark in the presence of 0.5% formaldehyde. In contrast, the *E. coli* K-12 derivatives CS109,

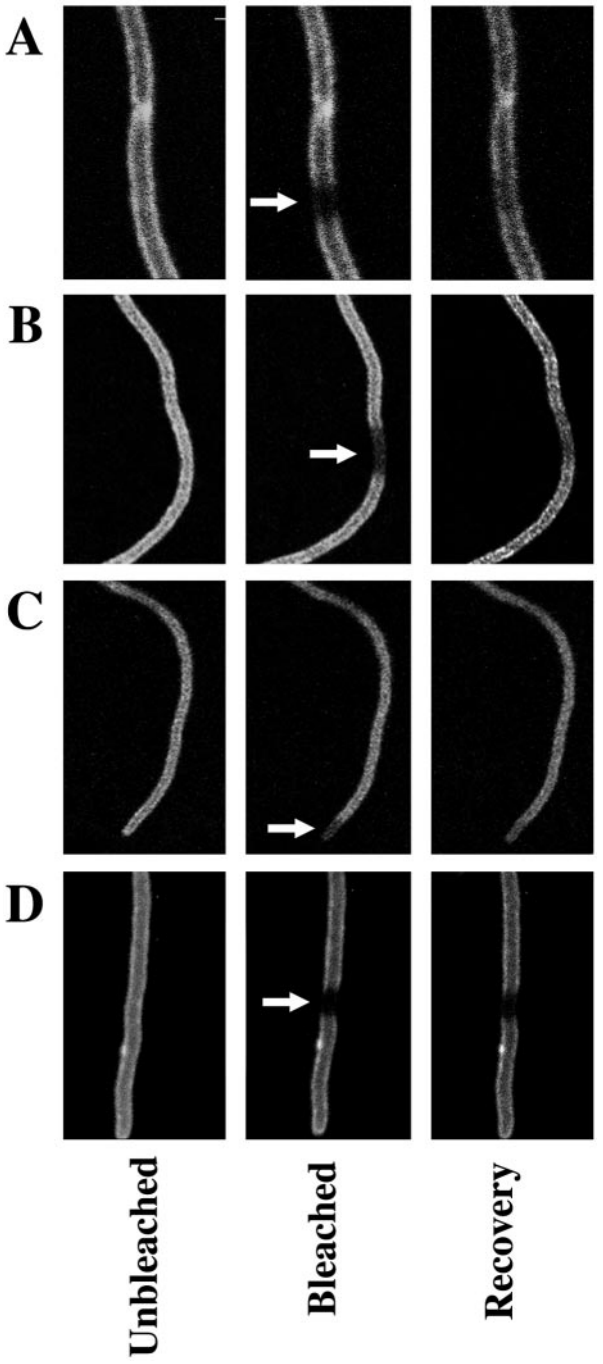

FIG. 2. FRAP analysis of protein and LPS diffusion in the OM. *E. coli* was filamented by treatment with aztreonam for 1 to 2 h, after which OM proteins were stained with NHS-AF488 (A to C) or the LPS O8 antigen was stained with ConA-AF488 (D). A segment of each filament was photobleached by laser exposure and photographed every 5 s for several minutes. The results for three time points are shown here for individual experiments. For each set, the left image is just prior to photobleaching, the center image is just after photobleaching, and the right image is 1 to 5 min after bleaching. As shown in Fig. 3, the extent of fluorescence recovery occurred quickly and was approximately equivalent at any time from 0.5 to 10 min after photobleaching. (A to C) *E. coli* CS109 proteins stained with NHS-AF488. (D) *E. coli* 2443 O8 antigen stained with ConA-AF488.

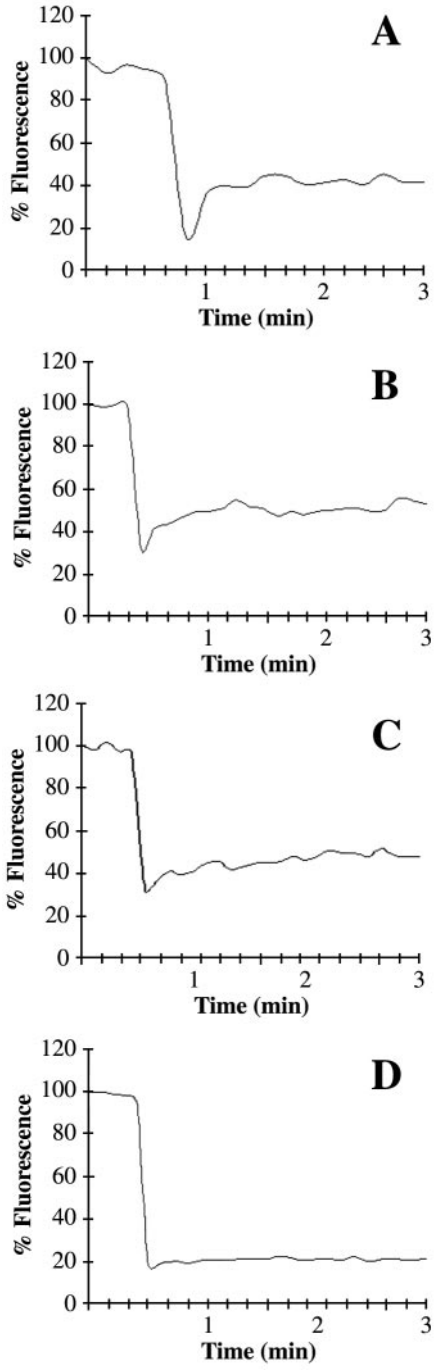

FIG. 3. Rates of FRAP for OM proteins and LPS. Panels A to D represent the time course of fluorescence recovery for the photobleached segments of cells in Fig. 2A to D. The steep drop in fluorescence denotes the time of laser exposure and photobleaching. The extent of fluorescence recovery remained stable from 3 min to over 10 min (not shown).

JM105, and KM32 did not retain ConA-AF488 after washing (Fig. 5B and Table 1). These results were consistent with the fact that K-12 strains do not express a complete O antigen (30), which we confirmed by observing O chains in the LPS profile of *E. coli* 2443 (Fig. 5C, lane 2) but not in *E. coli* CS109 (Fig. 5C, lane 3) or KM32 (Table 1).

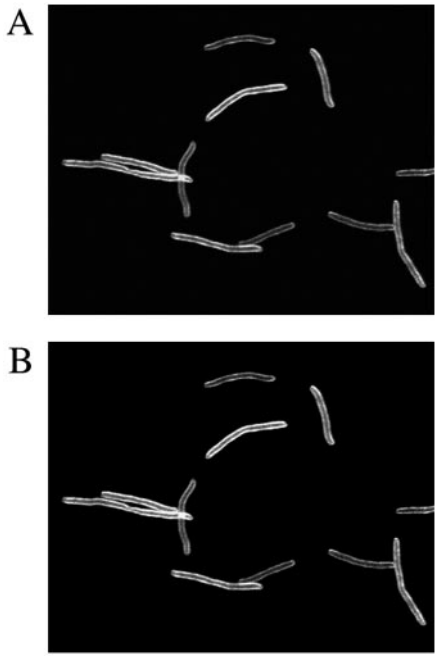

FIG. 4. Pulse-chase visualization of inner membrane stained with the lipophilic dye FM4-64. The inner membrane of *E. coli* CS109 was labeled with FM4-64, and stained cells were grown in the presence of aztreonam at 37°C for 60 min in the absence of label, harvested, and visualized by confocal microscopy. Panels: A, confocal image; B, image after processing by deconvolution.

To assure ourselves that the ConA-directed staining characteristics of *E. coli* 2443 reflected only the presence or absence of the O8 antigen, we moved the *rfb* genes of *E. coli* KM32 (a K-12 strain) into *E. coli* 2443 by phage P1 cotransduction with a closely linked kanamycin resistance marker, creating strain AG430-2K. To be certain that no additional mutations had been created, the $rfb_{\text{K-12}}$ genes were moved by a second cotransduction from AG430-2K into *E. coli* 2443T, creating strain AGTO2-1K. Both AG430-2K and AGTO2-1K lost the ability to synthesize O8-antigen side chains, as determined by SDS-polyacrylamide gel electrophoresis (PAGE) (not shown), and neither was stained by ConA-AF488 (Table 1), indicating that replacing the rfb_{O8} genes with their K-12 variants eliminated ConA binding.

The inability of K-12 strains to bind ConA seems at odds with observations that ConA agglutinates K-12 strains (45, 46) and immobilizes *E. coli* JM105 to lectin-derivatized membranes (15). However, a small number of molecules may agglutinate or immobilize whole cells, so such results do not prove that ConA binds uniformly to the OM. Consistent with the results presented here, Stoitsova et al. did not observe binding of gold-labeled ConA to *E. coli* K-12 (57). Thus, ConA may bind with low avidity to carbohydrate residues other than those of the O side chain, as is suggested by the lectin's ability to agglutinate *E. coli* serotypes having different O antigens (32). In any event, the ability to retain a substantial, visibly fluorescent ConA-linked dye was limited to cells expressing the O8 antigen, which contains repeated units of α-mannose (5).

Helical distribution of stable LPS. Having shown that ConA-AF488 specifically stains the O8 antigen of *E. coli* 2443,

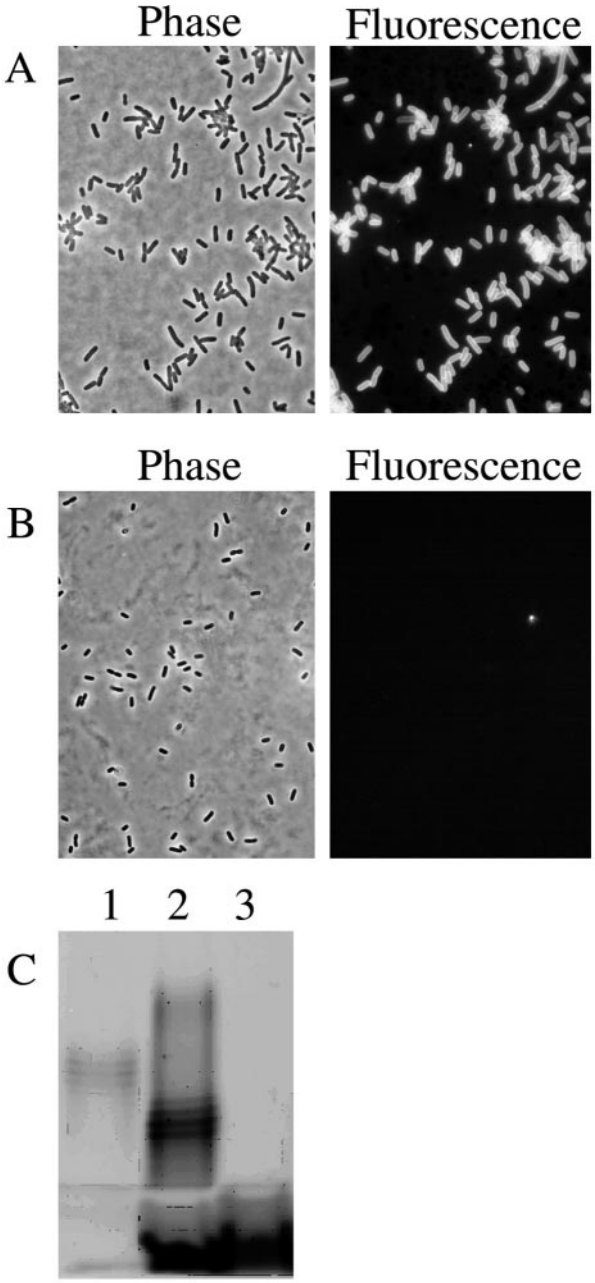

FIG. 5. Labeling and detection of LPS O8 antigen with ConA-AF488. (A and B) *E. coli* was stained with ConA-AF488, washed once in buffer lacking the dye, and examined by phase-contrast or fluorescence microscopy. Panels: A, *E. coli* 2443 (O8 antigen positive); B, *E. coli* CS109 (O-antigen-negative K-12 strain); C, LPS profiles of O-antigen-positive and -negative strains. LPS from *E. coli* was separated by SDS-PAGE as described in Materials and Methods and visualized with the Pro-Q Emerald LPS stain. Lanes: 1, control LPS preparation from *E. coli* serotype O55:B5; 2, LPS from *E. coli* 2443 (O8 antigen positive); 3, LPS from *E. coli* CS109 (O-antigen-negative K-12 strain). The series of evenly spaced bands represents variously sized O-antigen side chains in *E. coli* 2443 (lane 2) that are absent in *E. coli* CS109 (lane 3).

we used this reagent to determine how LPS was organized in the OM. When cells were labeled with ConA-AF488 and grown for two to four generations in the absence of the lectin, stable patches of fluorescently labeled O8 antigen were observed at the cell poles and in helical ribbons along the lateral walls (Fig. 6). Although helical strings could be observed in single cells by confocal microscopy (Fig. 6A), the LPS helices were visualized more sharply in filamentous cells by deconvoluting a set of *z* stack images (Fig. 6B and C). The results indicate that a subset of LPS molecules in the OM were not diluted by insertion of new material. Instead, they were immobilized in a specific geometric arrangement on the outer surface of the cell.

Previous experiments established that a relationship exists between the cell division initiator FtsZ and the synthesis of inert patches of peptidoglycan (10, 62). To determine if FtsZ polymerization contributed to the formation of the long-lived LPS domains, cells were elongated by expressing the FtsZ inhibitor SulA (40, 61). When SulA-induced cell filaments of *E. coli* 2443 were labeled with ConA-AF488 and chased, the same helical ribbons of stable O8 antigen were observed (Fig. 6C). Thus, generation of LPS helices did not require FtsZ polymerization.

The LPS helices appeared similar in extent and pitch to the stable protein helices in cells labeled with NHS-linked dyes. Although it seems reasonable that the two helices represent a single structure, the bleed-over emission of the bright Alexa-Fluor dye into the red emission channel prevented us from determining directly if the LPS and protein helices were coincident.

ConA-labeled LPS does not diffuse in the OM. One explanation for the appearance of LPS helices might be that the OM is composed of discrete "canals" that are kept separate from one another. LPS might freely diffuse in any one canal but be unable to cross into neighboring domains, thereby giving the illusion of stable swaths of LPS. We tested this idea by subjecting ConA-AF488-stained filaments to FRAP analysis. In 23 cases in which cells filaments were labeled but not chased, the bleached portion of the uniformly stained filament did not regain fluorescence even after 30 to 40 min of incubation (Fig. 2D and 3D and data not shown). When FRAP analysis was performed on cell filaments that had been labeled and chased so that LPS helices were visible, the same result was observed—LPS from the helices did not diffuse into the bleached areas (not shown). Thus, in contrast to OM proteins, ConA-labeled LPS did not diffuse freely within the OM.

ConA binding does not inhibit protein diffusion. It was possible that ConA binding might alter the diffusion properties of the OM. We tested this by labeling OM proteins of *E. coli* 2443 with NHS-AF488, binding unlabeled ConA to the O8 antigen on the surface of these same cells, and observing protein diffusion by FRAP. Labeled proteins returned to bleached areas at the same rate regardless of the presence or absence of ConA bound to LPS (not shown), indicating that ConA labeling did not significantly alter protein diffusion in the OM.

DISCUSSION

Bacteria are highly organized and architecturally complex. Several cytoplasmic proteins orient themselves and move along

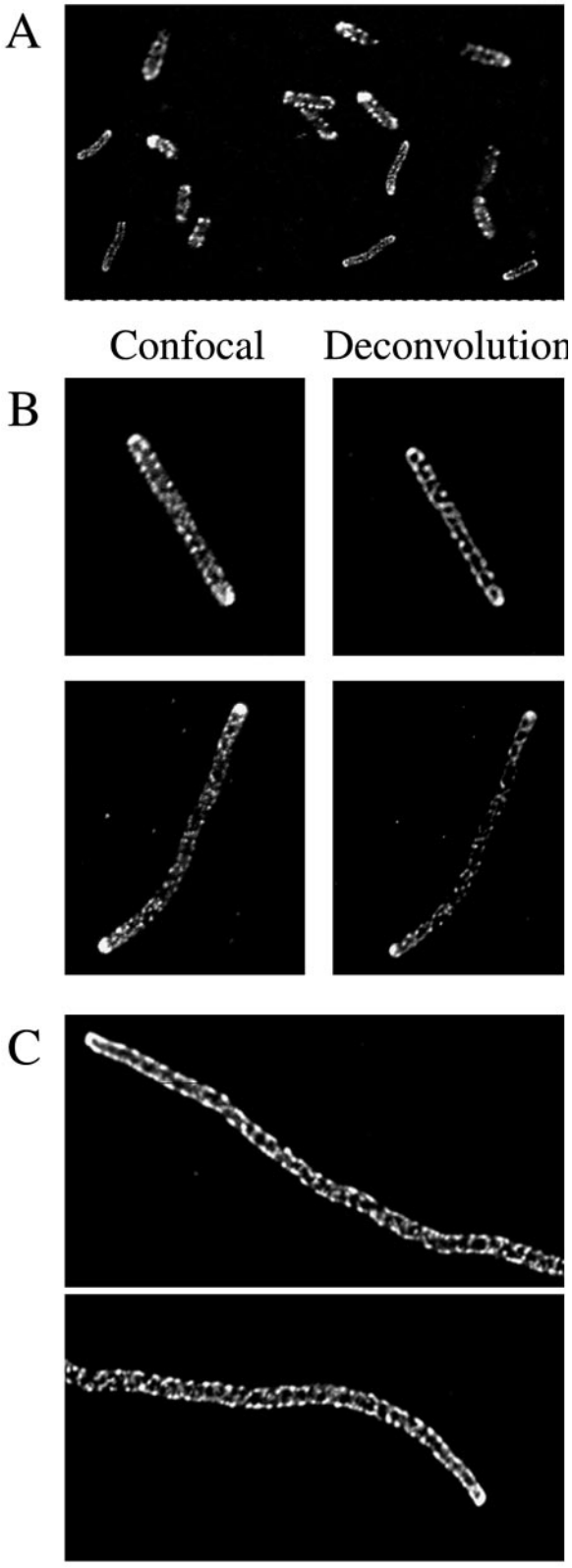

FIG. 6. Pulse-chase visualization of OM LPS helices in *E. coli* 2443. The O8 antigen of LPS in the OM was labeled with ConA-AF488. Stained cells were grown at 37°C in the absence of label, harvested, and visualized by confocal microscopy. Panels: A, original confocal image of cells stained with ConA-AF488 and then chased for 60 min in the absence of label; B, confocal and deconvolved images of cells filamented for 30 min with aztreonam, stained with ConA-AF488, and then chased for 60 min in the absence of label; C, deconvolved confocal image of a cell filamented by expression of SulA for 60 min, stained with ConA-AF488, and then chased for 60 min in the absence of label. The two images represent the full length of a single filamentous cell.

intricate helical pathways in the cytoplasm or along the inner face of the cytoplasmic membrane, and the cell poles appear to be organelle-like domains consisting of long-lived patches of peptidoglycan and membrane proteins. To these patterns we now add the observation that LPS and proteins form stable domains not only at the poles but also along one or more helical ribbons within the OM of *E. coli*. Thus, this part of the envelope is not homogeneous but instead exhibits subtle structural variations. The cell's emphasis on creating privileged sites and populating them with specific proteins suggests that these elaborate structures serve fundamental purposes, so it is important to understand the mechanisms responsible for their existence. The present results have implications for the in vivo behavior of LPS, the distribution of OM proteins, and envelope synthesis.

LPS stability versus diffusion. The inability of ConA-labeled LPS to diffuse into bleached areas of the OM raises the question of why LPS should exhibit such stability. An extensive literature supports the existence of strong bonds between neighboring LPS molecules (42, 43). For example, in artificial membrane vesicles stable islands of LPS persist for days in a "sea of phospholipid," indicating the existence of extremely durable lateral interactions between LPS molecules (59). Also, hexagonal arrays of tightly packed LPS subunits are observed in electron micrographs of crystallized LPS (24, 64) and by X-ray crystallography and atomic force microscopy (25). Four forces generate this high degree of organization: van der Waals attractions between fatty acid chains, bridging of LPS molecules by divalent cations, hydrogen bonding, and interactions between the O polysaccharides of neighboring molecules (2, 23, 27, 42).

Several groups have rationalized these observations by three-dimensional molecular modeling. In the model of Kastowsky et al., the structure of the LPS inner and outer cores are rigid and well defined but the O side chain is flexible and can adopt many conformations (23). The most energetically favorable predicts that the O polysaccharide is bent into an "L" shape, folded over and lying parallel to the membrane surface, and in contact with the head groups of neighboring LPS molecules or membrane-embedded proteins (23). The authors concluded that the variety of intermolecular contacts would allow the O polysaccharide to self-assemble as "a mechanically stable, feltlike network" (23). A similar conclusion is supported by modeling that indicates that a single LPS molecule, viewed from above, is shaped like a triangular wedge or pie slice (64). Six such molecules can self-associate with their points facing inward to form a circular hexamer, and multiple hexamers can form a regular hexagonal lattice held together by divalent cations (27, 64). Brandenburg and Wiese reemphasize the importance of these interactions, although they believe that the aqueous gaps between the LPS hexamers might not be favored in vivo (2). Overall, several experimental and computational

reasons support the idea that the bonds between neighboring LPS molecules are strong and directional. It should be remembered, however, that these structural studies and modelings were performed on membranes of pure LPS when, in fact, the OM is full of proteins whose presence would interrupt any strictly regular geometric arrangement of an LPS-only leaflet.

None of the above considerations indicates whether LPS molecules diffuse freely among themselves. Schindler et al. addressed this question directly by incorporating exogenous rhodamine-labeled LPS into the OM of *Salmonella enterica* serovar Typhimurium (53). FRAP analysis in cell filaments indicated that LPS diffused freely with no immobile components (53). Mühlradt et al. reached essentially the same conclusion by using antibodies to determine the fate of newly inserted LPS (39). Both of these results are the opposite of what we report here, in that we saw little or no LPS diffusion into bleached areas in FRAP experiments. However, significant differences in the experimental approaches used may explain the disparities. Schindler et al. (53) labeled LPS with rhodamine isothiocyanate, which cross-links to amines located in the inner core of LPS. Addition of the bulky aromatic dye probably disrupts important hydrogen bonds, and the accompanying steric hindrance may prevent bridging by divalent cations (23). These alterations would seriously impair LPS-LPS interactions so that the labeled compound would diffuse more readily than normal. In fact, Schindler et al. (53) calculated an LPS diffusion rate that is ~1,000 times faster than that determined by Mühlradt et al., who performed their experiments with wild-type cells expressing an LPS with longer O-antigen side chains (38, 39). The latter group labeled LPS with antibody and inferred the extent of LPS dispersal by using electron microscopy. They concluded that LPS diffuses at least 10,000 times less rapidly than do other membrane phospholipids (38). Even so, Gibbs et al. recently produced evidence that the OM protein LamB is distributed differently in live cells than in fixed cells, which they ascribe to redistribution caused by chemical fixation (20). Susceptibility to this artifact suggests that LPS may diffuse even more slowly in vivo than the already low rate reported by Mühlradt et al.

The preceding rate estimates may be sufficient to explain why we observed little or no LPS diffusion. However, an additional consideration may apply to our results. Because ConA exists as tetramers at pH >7.0 (8), the multivalent lectin might cross-link neighboring molecules so that native LPS-LPS interactions are enhanced by the labeling system itself. The strength of these combined stabilizing forces could reduce or prevent normal LPS diffusion. On the other hand, even after labeling with ConA, LPS-LPS interactions were not so strong as to inhibit insertion of new material during pulse-chase experiments or to inhibit protein diffusion. Thus, any ConA-enhanced LPS interaction was neither overpowering nor permanent. Therefore, although we cannot conclude that LPS is completely immobile, its natural diffusion rate must be quite small.

Diffusion of OM proteins and polar stability. Unlike LPS, at least some proteins diffused freely in the OM to repopulate bleached areas. This diffusion was not affected appreciably by binding of unlabeled ConA to the O8 antigen, so even if the lectin did cross-link neighboring LPS molecules it did not impact protein movement. Because proteins in helical structures were stable over several generations, it seems that OM proteins must be grouped into mobile and immobile populations. We cannot tell if the populations are composed of different proteins or if the immobile group is a subpopulation of the whole.

One place where this mobile-immobile dichotomy is very clear and potentially informative is at the cell poles. Peptidoglycan and the overlying LPS and OM proteins are retained at the poles even after several generations of growth (9, 12). Nonetheless, OM proteins diffused into and out of these polar regions at a rate equal to or only very slightly less than the rate at which they diffused throughout the side wall. This is consistent with previous observations that the IcsA protein, which is secreted to the OM specifically at the poles, moves from there to cover the entire bacterial surface (50, 52). The conclusion must be that there is no impenetrable barrier blocking protein diffusion between the poles and side walls. The most likely alternative for explaining protein stability at the poles is that some proteins are tethered to one or more polar components, with inert peptidoglycan being the most prominent candidate. Noncovalent peptidoglycan binding domains, such as that found in OmpA (63), and covalent attachments, as exemplified by Braun's lipoprotein (47), might contribute the necessary anchors to immobilize one or more proteins.

Helical structure of the OM. The pulse-chase experiments with labeled proteins and LPS revealed a new structural element in the gram-negative envelope. Despite the free diffusion of bulk OM proteins, chased cells accumulated long-lived ribbons of protein wrapped around the cell in a helical manner. Similarly, swaths of ConA-labeled LPS maintained long-lived associations over several generations of growth, indicating that the molecules were neither diluted by insertion of new material nor removed or recycled.

A simple way to approach the question of how such protein and LPS helices survive is to envision an "insertion barrier" that prevents addition of new molecules into these ribbons. One possibility is that during the chase period LPS is inserted between ConA-labeled molecules but then, as sufficient numbers of unlabeled molecules accumulate, new material is inserted preferentially between unlabeled LPS molecules. If ConA-enhanced LPS-LPS interactions tilt the balance of insertion toward non-ConA-linked domains, then the surviving helices would be artifacts generated by a mechanism that indirectly preserves swaths of ConA-labeled material. If this is true, then the ConA-labeled ribbons would reflect the geometry of the initial stages of OM synthesis, implying that insertion of new envelope material runs along one or more helical tracks.

An alternate explanation is that the helical ribbons of protein or LPS represent fixed domains that are naturally impervious, so that insertion of new material occurs only between ribbons. Addition of newly synthesized proteins or LPS would dilute labeled molecules in the insertion zones, creating darker areas as the cell grows, but would not dilute label in the impervious zones, leaving the observed ribbons. If this interpretation is correct, then the helical structures would represent permanent components of the OM. In this case, synthesis of most of the OM might or might not proceed via a helical mechanism; only synthesis of the inert portion of the envelope would have to be helical. For the rest of the envelope, LPS

insertion into the OM could be diffuse and random within broad zones between the inert boundaries, so that any departure from complete randomness might be so slight as to be overlooked by previous techniques. If these zones were bounded by persistent helical ribbons, diffusion of lipids or proteins could be confined to spiral canals that loop around the OM, possibly accounting for the helical diffusion of LamB (20).

As discussed above in relation to cell poles, a possible mechanical explanation for the stability of OM helices is that one or more components are riveted to an underlying spiral arrangement of inert cell wall, producing a tightly linked sandwich of peptidoglycan, LPS, and proteins that resists attempts to insert new material. In this scenario, the geometry of the ConA- or NHS-labeled ribbons would reflect the underlying distribution of inert peptidoglycan. By evaluating the distribution of newly inserted peptidoglycan precursors, de Pedro et al. produced images suggesting that older peptidoglycan is distributed as helical ribbons in the side wall of *E. coli* (11). Also, peptidoglycan is incorporated into the cell wall of *B. subtilis* in helical tracks (7), although it is not known whether these are stable over time. Although these findings are consistent with the idea that the three envelope components could be interconnected, it is not technically feasible to visualize whether the inert peptidoglycan helices are coincident with the LPS and protein helices we observe. In summary, the observed distribution of stable LPS ribbons could be the product of an underlying helical mechanism that governs either LPS insertion or peptidoglycan synthesis and envelope attachment.

O-antigen labeling. As a final technical note, the use of fluorescently labeled ConA to screen for the presence, absence, or distribution of the O8 antigen should be useful for other applications as well. ConA labeling represents a simple in vivo screen for the presence in *E. coli* and *Salmonella* species of O antigens that contain α-mannose (51), and lectins with different specificities should be useful for monitoring the presence of alternate O-polysaccharide side chains.

ACKNOWLEDGMENTS

We especially thank Tamara J. Casavan for instruction and help in operating the confocal microscope and John Lee for assembling the graphics.

This work was supported by grant GM061019 from the National Institutes of Health.

ADDENDUM IN PROOF

After this paper was accepted, we were able to disentangle the fluorescent emissions of the two dyes in double-labeled cells by spectral imaging of samples observed by confocal microscopy. The results demonstrated that the stable outer membrane helices of Texas red-stained proteins and Alexa-Fluor-stained LPS were coincident with one another, implying that the proteins and LPS are components of a common helical structure in the outer membrane (B. M. Meberg and K. D. Young, unpublished data).

REFERENCES

1. **Ben-Yehuda, S., D. Z. Rudner, and R. Losick.** 2003. RacA, a bacterial protein that anchors chromosomes to the cell poles. Science **299:**532–536.
2. **Brandenburg, K., and A. Wiese.** 2004. Endotoxins: relationships between structure, function, and activity. Curr. Top. Med. Chem. **4:**1127–1146.
3. **Brandon, L. D., N. Goehring, A. Janakiraman, A. W. Yan, T. Wu, J. Beckwith, and M. B. Goldberg.** 2003. IcsA, a polarly localized autotransporter with an atypical signal peptide, uses the Sec apparatus for secretion, although the Sec apparatus is circumferentially distributed. Mol. Microbiol. **50:**45–60.
4. **Campo, N., H. Tjalsma, G. Buist, D. Stepniak, M. Meijer, M. Veenhuis, M. Westermann, J. P. Muller, S. Bron, J. Kok, O. P. Kuipers, and J. D. Jongbloed.** 2004. Subcellular sites for bacterial protein export. Mol. Microbiol. **53:**1583–1599.
5. **Clarke, B. R., L. Cuthbertson, and C. Whitfield.** 2004. Nonreducing terminal modifications determine the chain length of polymannose O antigens of *Escherichia coli* and couple chain termination to polymer export via an ATP-binding cassette transporter. J. Biol. Chem. **279:**35709–35718.
6. **Cowan, A. E., E. M. Olivastro, D. E. Koppel, C. A. Loshon, B. Setlow, and P. Setlow.** 2004. Lipids in the inner membrane of dormant spores of *Bacillus* species are largely immobile. Proc. Natl. Acad. Sci. USA **101:**7733–7738.
7. **Daniel, R. A., and J. Errington.** 2003. Control of cell morphogenesis in bacteria. Two distinct ways to make a rod-shaped cell. Cell **113:**767–776.
8. **Debenham, S. D., P. W. Snyder, and E. J. Toone.** 2003. Solid-phase synthesis for the identification of high-affinity bivalent lectin ligands. J. Org. Chem. **68:**5805–5811.
9. **de Pedro, M. A., C. G. Grunfelder, and H. Schwarz.** 2004. Restricted mobility of cell surface proteins in the polar regions of *Escherichia coli*. J. Bacteriol. **186:**2594–2602.
10. **de Pedro, M. A., J. C. Quintela, J.-V. Höltje, and H. Schwarz.** 1997. Murein segregation in *Escherichia coli*. J. Bacteriol. **179:**2823–2834.
11. **de Pedro, M. A., H. Schwarz, and A. L. Koch.** 2003. Patchiness of murein insertion into the sidewall of *Escherichia coli*. Microbiology **149:**1753–1761.
12. **de Pedro, M. A., K. D. Young, J.-V. Höltje, and H. Schwarz.** 2003. Branching of *Escherichia coli* cells arises from multiple sites of inert peptidoglycan. J. Bacteriol. **185:**1147–1152.
13. **Ebersbach, G., and K. Gerdes.** 2004. Bacterial mitosis: partitioning protein ParA oscillates in spiral-shaped structures and positions plasmids at mid-cell. Mol. Microbiol. **52:**385–398.
14. **Edwards, D. H., and J. Errington.** 1997. The *Bacillus subtilis* DivIVA protein targets to the division septum and controls the site specificity of cell division. Mol. Microbiol. **24:**905–915.
15. **Ertl, P., and S. R. Mikkelsen.** 2001. Electrochemical biosensor array for the identification of microorganisms based on lectin-lipopolysaccharide recognition. Anal. Chem. **73:**4241–4248.
16. **Espeli, O., P. Nurse, C. Levine, C. Lee, and K. J. Marians.** 2003. SetB: an integral membrane protein that affects chromosome segregation in *Escherichia coli*. Mol. Microbiol. **50:**495–509.
17. **Figge, R. M., A. V. Divakaruni, and J. W. Gober.** 2004. MreB, the cell shape-determining bacterial actin homologue, co-ordinates cell wall morphogenesis in *Caulobacter crescentus*. Mol. Microbiol. **51:**1321–1332.
18. **Fishov, I., and C. L. Woldringh.** 1999. Visualization of membrane domains in *Escherichia coli*. Mol. Microbiol. **32:**1166–1172.
19. **Flardh, K.** 2003. Essential role of DivIVA in polar growth and morphogenesis in Streptomyces coelicolor $A3_2$. Mol. Microbiol. **49:**1523–1536.
20. **Gibbs, K. A., D. D. Isaac, J. Xu, R. W. Hendrix, T. J. Silhavy, and J. A. Theriot.** 2004. Complex spatial distribution and dynamics of an abundant *Escherichia coli* outer membrane protein, LamB. Mol. Microbiol. **53:**1771–1783.
21. **Hitchcock, P. J., and T. M. Brown.** 1983. Morphological heterogeneity among *Salmonella* lipopolysaccharide chemotypes in silver-stained polyacrylamide gels. J. Bacteriol. **154:**269–277.
22. **Jones, L. J., R. Carballido-Lopez, and J. Errington.** 2001. Control of cell shape in bacteria: helical, actin-like filaments in *Bacillus subtilis*. Cell **104:**913–922.
23. **Kastowsky, M., T. Gutberlet, and H. Bradaczek.** 1992. Molecular modeling of the three-dimensional structure and conformational flexibility of bacterial lipopolysaccharide. J. Bacteriol. **174:**4798–4806.
24. **Kato, N., M. Ohta, N. Kido, H. Ito, S. Naito, T. Hasegawa, T. Watabe, and K. Sasaki.** 1990. Crystallization of R-form lipopolysaccharides from *Salmonella minnesota* and *Escherichia coli*. J. Bacteriol. **172:**1516–1528.
25. **Kato, N., T. Sugiyama, S. Naito, Y. Arakawa, H. Ito, N. Kido, M. Ohta, and K. Sasaki.** 2000. Molecular structure of bacterial endotoxin (*Escherichia coli* Re lipopolysaccharide): implications for formation of a novel heterogeneous lattice structure. Mol. Microbiol. **36:**796–805.
26. **Koch, A. L., and C. L. Woldringh.** 1994. The metabolic inertness of the pole wall of a gram-negative rod. J. Theor. Biol. **171:**415–425.
27. **Kotra, L. P., D. Golemi, N. A. Amro, G.-Y. Liu, and S. Mobashery.** 1999. Dynamics of the lipopolysaccharide assembly on the surface of *Escherichia coli*. J. Am. Chem. Soc. **121:**8707–8711.
28. **Kristensen, C. S., L. Eberl, J. M. Sanchez-Romero, M. Givskov, S. Molin, and V. de Lorenzo.** 1995. Site-specific deletions of chromosomally located DNA segments with the multimer resolution system of broad-host-range plasmid RP4. J. Bacteriol. **177:**52–58.
29. **Kroos, L., and J. R. Maddock.** 2003. Prokaryotic development: emerging insights. J. Bacteriol. **185:**1128–1146.
30. **Liu, D., and P. R. Reeves.** 1994. *Escherichia coli* K12 regains its O antigen. Microbiology **140**(Pt. 1)**:**49–57.

31. **Lybarger, S. R., and J. R. Maddock.** 2001. Polarity in action: asymmetric protein localization in bacteria. J. Bacteriol. **183:**3261–3267.
32. **Mangia, A. H., E. B. Bergter, L. M. Teixeira, and F. C. Silva Filho.** 1999. A preliminary investigation on the chemical composition of the cell surface of five enteropathogenic *Escherichia coli* serotypes. Mem. Inst. Oswaldo Cruz **94:**513–518.
33. **Margolin, W.** 2003. Bacterial shape: growing off this mortal coil. Curr. Biol. **13:**R705–R707.
34. **Meberg, B. M., A. L. Paulson, R. Priyadarshini, and K. D. Young.** 2004. Endopeptidase penicillin binding proteins 4 and 7 play auxiliary roles in determining uniform morphology of *Escherichia coli*. J. Bacteriol. **186:**8326–8336.
35. **Meier, U., and H. Mayer.** 1985. Genetic location of genes encoding enterobacterial common antigen. J. Bacteriol. **163:**756–762.
36. **Miller, J. H.** 1972. Experiments in molecular genetics. Cold Spring Harbor Laboratory, Cold Spring Harbor, N.Y.
37. **Miller, J. H.** 1992. A short course in bacterial genetics: a laboratory manual and handbook for *Escherichia coli* and related bacteria. Cold Spring Harbor Laboratory Press, Plainview, N.Y.
38. **Mühlradt, P. F., J. Menzel, J. R. Golecki, and V. Speth.** 1974. Lateral mobility and surface density of lipopolysaccharide in the outer membrane of *Salmonella typhimurium*. Eur. J. Biochem. **43:**533–539.
39. **Mühlradt, P. F., J. Menzel, J. R. Golecki, and V. Speth.** 1973. Outer membrane of *Salmonella*: sites of export of newly synthesised lipopolysaccharide on the bacterial surface. Eur. J. Biochem. **35:**471–481.
40. **Mukherjee, A., C. N. Cao, and J. Lutkenhaus.** 1998. Inhibition of FtsZ polymerization by SulA, an inhibitor of septation in *Escherichia coli*. Proc. Natl. Acad. Sci. USA **95:**2885–2890.
41. **Murphy, K. C.** 1998. Use of bacteriophage lambda recombination functions to promote gene replacement in *Escherichia coli*. J. Bacteriol. **180:**2063–2071.
42. **Nikaido, H.** 2003. Molecular basis of bacterial outer membrane permeability revisited. Microbiol. Mol. Biol. Rev. **67:**593–656.
43. **Nikaido, H.** 1996. Outer membrane, p. 29–47. *In* F. C. Neidhardt, R. Curtiss III, J. L. Ingraham, E. C. C. Lin, K. B. Low, B. Magasanik, W. S. Reznikoff, M. Riley, M. Schaechter, and H. E. Umbarger (ed.), *Escherichia coli* and *Salmonella*: cellular and molecular biology, 2nd ed., vol. 1. ASM Press, Washington, D.C.
44. **Nilsen, T., A. S. Ghosh, M. B. Goldberg, and K. D. Young.** 2004. Branching sites and morphological abnormalities behave as ectopic poles in shape-defective *Escherichia coli*. Mol. Microbiol. **52:**1045–1054.
45. **Picken, R., and I. R. Beacham.** 1975. The interaction of concanavalin A with mutant and wild-type strains of *Escherichia coli* K12. Biochem. Soc. Trans. **3:**387–388.
46. **Picken, R. N., and I. R. Beacham.** 1977. Bacteriophage-resistant mutants of *Escherichia coli* K12 with altered lipopolysaccharide. Studies with concanavalin A. J. Gen. Microbiol. **102:**319–326.
47. **Pittenauer, E., J. C. Quintela, E. R. Schmid, G. Allmaier, G. Paulus, and M. A. de Pedro.** 1995. Characterization of Braun's lipoprotein and determination of its attachment sites to peptidoglycan by ^{252}Cf-PD and MALDI time-of-flight mass spectrometry. J. Am. Soc. Mass Spectrom. **6:**892–905.
48. **Raetz, C. R., and C. Whitfield.** 2002. Lipopolysaccharide endotoxins. Annu. Rev. Biochem. **71:**635–700.
49. **Raetz, C. R. H.** 1996. Bacterial lipopolysaccharides: a remarkable family of bioactive macroamphiphiles, p. 1035–1063. *In* F. C. Neidhardt, R. Curtiss III, J. L. Ingraham, E. C. C. Lin, K. B. Low, B. Magasanik, W. S. Reznikoff, M. Riley, M. Schaechter, and H. E. Umbarger (ed.), *Escherichia coli* and *Salmonella*: cellular and molecular biology, 2nd ed., vol. 1. ASM Press, Washington, D.C.
50. **Robbins, J. R., D. Monack, S. J. McCallum, A. Vegas, E. Pham, M. B. Goldberg, and J. A. Theriot.** 2001. The making of a gradient: IcsA (VirG) polarity in *Shigella flexneri*. Mol. Microbiol. **41:**861–872.
51. **Samuel, G., and P. Reeves.** 2003. Biosynthesis of O-antigens: genes and pathways involved in nucleotide sugar precursor synthesis and O-antigen assembly. Carbohydr. Res. **338:**2503–2519.
52. **Sandlin, R. C., M. B. Goldberg, and A. T. Maurelli.** 1996. Effect of O side-chain length and composition on the virulence of *Shigella flexneri* 2a. Mol. Microbiol. **22:**63–73.
53. **Schindler, M., M. J. Osborn, and D. E. Koppel.** 1980. Lateral diffusion of lipopolysaccharide in the outer membrane of *Salmonella typhimurium*. Nature **285:**261–263.
54. **Shapiro, L.** 1993. Protein localization and asymmetry in the bacterial cell. Cell **73:**841–855.
55. **Shapiro, L., H. H. McAdams, and R. Losick.** 2002. Generating and exploiting polarity in bacteria. Science **298:**1942–1946.
56. **Shih, Y. L., T. Le, and L. Rothfield.** 2003. Division site selection in *Escherichia coli* involves dynamic redistribution of Min proteins within coiled structures that extend between the two cell poles. Proc. Natl. Acad. Sci. USA **100:**7865–7870.
57. **Stoitsova, S., R. Ivanova, and I. Dimova.** 2004. Lectin-binding epitopes at the surface of *Escherichia coli* K-12: examination by electron microscopy, with special reference to the presence of a colanic acid-like polymer. J. Basic Microbiol. **44:**296–304.
58. **Sun, Q., and W. Margolin.** 1998. FtsZ dynamics during the division cycle of live *Escherichia coli* cells. J. Bacteriol. **180:**2050–2056.
59. **Takeuchi, Y., and H. Nikaido.** 1981. Persistence of segregated phospholipid domains in phospholipid-lipopolysaccharide mixed bilayers: studies with spin-labeled phospholipids. Biochemistry **20:**523–529.
60. **Thanedar, S., and W. Margolin.** 2004. FtsZ exhibits rapid movement and oscillation waves in helix-like patterns in *Escherichia coli*. Curr. Biol. **14:**1167–1173.
61. **Trusca, D., S. Scott, C. Thompson, and D. Bramhill.** 1998. Bacterial SOS checkpoint protein SulA inhibits polymerization of purified FtsZ cell division protein. J. Bacteriol. **180:**3946–3953.
62. **Varma, A., and K. D. Young.** 2004. FtsZ collaborates with penicillin binding proteins to generate bacterial cell shape in *Escherichia coli*. J. Bacteriol. **186:**6768–6774.
63. **Wang, Y.** 2002. The function of OmpA in *Escherichia coli*. Biochem. Biophys. Res. Commun. **292:**396–401.
64. **Wang, Y., and R. I. Hollingsworth.** 1996. An NMR spectroscopy and molecular mechanics study of the molecular basis for the supramolecular structure of lipopolysaccharides. Biochemistry **35:**5647–5654.